JEE Journal of Ecological Engineering

Journal of Ecological Engineering, 2025, 26(10), 144–155
https://doi.org/10.12911/22998993/205747
ISSN 2299–8993, License CC-BY 4.0

Received: 2025.05.24
Accepted: 2025.07.15
Published: 2025.07.22

Synthesis and characterization of magnetic nanoparticles coated with citric acid as a coagulant for the Tigris River treatment

Miqat Hasan Salih[1]

[1] Department of Chemical Engineering, College of Engineering, University of Baghdad, Baghdad, Iraq
E-mail: mekat.hassan@coeng.uobaghdad.edu.iq

ABSTRACT

The coagulation and flocculation process using coated magnetic nanoparticles is considered one of the effective technologies for turbidity removal. This study investigates an application of magnetic nanoparticles coated with citric acid in the coagulation and flocculation process on Tigris River water in Baghdad, Iraq. Magnetic nanoparticles (MNP1) were synthesized by the co-precipitation method and coated with citric acid (MNP2). The prepared MNP1 and MNP2 were characterized by XRD, FTIR, AFM, FE-SEM, EDS, and zeta potential analysis. For coagulation process, the effect of different types of coagulants (alum, $FeCl_3$, MNP1, MNP2), coagulant dosage (10–110 mg/l), and initial pH (3–9) were examined in this work. The best coagulant was MNP2 with zeta potential of -34.04 mV. The maximum removal efficiency for MNP2 at optimum dosage of 30 mg/l dosage was 96.72%. This value corresponds to the best value of initial pH of 6.

Keywords: MNPs, Tigris river, citric acid coated MNPs, turbidity removal, coagulation and flocculation.

INTRODUCTION

In recent years, the value of global water resources has increased significantly due to the continuous growth of the global population and the accelerated development of society. Of the 70% of the Earth that is covered by water, only 2.5% is freshwater, and the available freshwater resources are exceedingly scarce (Dhakal et al., 2022; Hu et al., 2024). There are a lot of undesirable impacts caused by the high turbidity levels found in most surface water resources used for drinking water (Mardani et al., 2021). Polluting rivers, lakes, and reservoirs are the byproducts of agricultural and animal facilities. These include nutrients, fertilizers, siltation, pesticides, metals, and diseases (Chhetri et al., 2022).

The possible interaction with downstream treatment processes and unfavorable impacts on consumer acceptance make effective reduction of turbidity one of the key aims in effective drinking water treatment. The filter can become prematurely clogged due to turbidity, which would disrupt the filtration process. Customers may be put off by the appearance of cloudiness in finished water, leading them to believe it is not clean or safe to drink. This is only one way in which turbidity affects water acceptance (Soros et al., 2019). For water that will be disinfected, the World Health Organization recommends < 1 NTU turbidity, while water that is acceptable to the human eye requires < 4 NTU (Organization, 2011).

Two major rivers, the Tigris and the Euphrates, pass through Iraq. The industrial, agricultural, and domestic sectors all make use of river water in some way. Due to wastewater discharge from towns and businesses, river water quality has been dropping, especially in the last 30 years (Ali Abed et al., 2019; Al-Madhhachi et al., 2020; Salih et al., 2024). Therefore, the water needs to undergo sufficient physical, chemical, and technological processing to meet quality standards (Salih et al., 2021).

Direct filtration, coagulation/settling treatment methods, membrane-based systems (Dhamin and Majeed, 2022; Al-tamimi et al., 2025),

and adsorption-based systems (Ahmed et al., 2021) are commonly used to remove organic matter (including SOCs), suspended particles, turbidity, and raw water sources from these sources. Nevertheless, there is no single, cost-effective, and efficient water treatment process. By employing alum- or polymer-based coagulants to eliminate turbidity, color, organic matter, and other contaminants, numerous drinking water treatment facilities implement flocculation and coagulation systems (Chhetri et al., 2022). Coagulation has been considered one of the general methods for removing turbidity during wastewater treatment due to its minimal capital and operational costs (Zhou et al., 2017; Msemwa et al., 2025).

Traditional coagulation and flocculation methods may be implemented to eliminate a substantial quantity of organic matter, oil, and suspended solids (Al-Rubaie et al., 2015; Mohammed and Shakir, 2018). The process of coagulation is the process by which suspended particulates and colloids are destabilized to facilitate their aggregation. The process is defined as the destabilization and charge neutralization of the particle as a result of the addition of a positively charged ion of metal salt or polyelectrolyte (Alwared and Faraj, 2015; Abdulameer and Makki, 2016). When particles that have coagulated come together, they form larger flocs, a process known as flocculation. Flocs are removed by sedimentation because their density is higher than water's (Farajnezhad and Gharbani, 2012; Jamaly et al., 2015; Mohammed and Abbas, 2017; Salih et al., 2021). Coagulation and flocculation process could be a pretreatment for reverse osmosis (Algureiri and Abdulmajeed, 2016), forward osmosis (Kadhim et al., 2024), pressure retarded osmosis (Salih et al., 2024), crystallization (Salih and Al-Alawy, 2022), and zero liquid discharge systems (Mohammadtabar et al., 2019). In most cases, alum ($Al_2(SO_4)_3$) or ferric chloride ($FeCl_3$) are used for this purpose (Mustereț et al., 2021; Msemwa et al., 2025).

The basic scientific interest in magnetic nanoparticles and their wide-ranging practical applications have led to their rapid development. Nanomaterials based on magnetic principles are now very desirable due to their increased surface area, small size, and wide range of potential uses (Stiufiuc & Stiufiuc, 2024; Deivasigamani et al., 2025; Khujamberdiev and Cho, 2025). Among the many novel properties of iron oxide nanoparticles (MNP) include their homogeneous size distribution, high magnetic permeability, large surface area, low cost, bioactivity, reduced toxicity, ease of recycling, and enrichment by magnetic separation (Chen et al., 2016; Deivasigamani et al., 2025).

Rather than using traditional coagulation, magnetic coagulation is now used to treat wastewater because of its exceptional properties. A new development in coagulation technology, magnetic seeds are introduced during the procedure. Magnetic seeds, which resemble small suspended particles, serve as coagulation nuclei by raising the effective collision rate of particles; hence, magnetic particle addition improves floc aggregation and coagulation efficiency. As a result of the forces exerted by Johannes van der Waals, colloidal particles and magnetic powder particles agglomerate together. Adsorption and bridging of flocculants cause the flocs to agglutinate and grow even more. Flocculants, magnetic seeds, and pollutants all come together to produce magnetic complexes, which enhance the efficacy of pollutant removal. Subsequently, a magnetic separation device may recycle the magnetic seeds, lowering the material cost, and great specific gravity and quick sedimentation allow for solid-liquid separation (Demissie et al., 2021; Ritigala, Chen, et al., 2021; Gao et al., 2022; Mohamed Noor et al., 2022).

Magnetic coagulation technology has been widely used in water treatment due to its many advantages. These include a large treatment capacity, low energy consumption, high treatment efficiency, simple operation, low sludge yield, and a significant reduction of follow-up load (Chen et al., 2016; Hatamie et al., 2016; Cai et al., 2018; Lv et al., 2021; Ritigala, Demissie, et al., 2021; Gao et al., 2022). Coagulation and flocculation technologies are improved as well by MNPs inclusion. Even at low dosages, coagulant/focculant(s) functionalized with MNPs have been shown to increase the efficiency of water treatment. An external magnetic field can be employed to achieve entire recovery of used/exhausted magnetic coagulant/focculant and to shorten settling time (Chen et al., 2019; Mohamed Noor et al., 2022). Given all these benefits, water treatment technology employing magnetic coagulant/focculants has received increasing attention from researchers and professionals (Mohamed Noor et al., 2022).

This study aims to synthesis of magnetic nanoparticles Fe_3O_4 (MNP1) by co-precipitation method and magnetic nanoparticles coated with

citric acid (MNP2) to extract pure water from the Tigris River in Baghdad City in Iraq by using the coagulation and flocculation process. Using these materials in a coagulation and flocculation process was the first attempt to purify water from the Tigris River. Water scarcity makes clean water all the more crucial in Iraq. The current study highlights the efficiency of the MNP1 and MNP2 in producing pure water by coagulation and flocculation process and compares the efficiency with traditional coagulants. The coagulant dosage and pH were studied. The efficiency was evaluated according to turbidity and removal efficiency.

EXPERIMENTAL WORK

Materials

$FeCl_3.6H_2O$ (98%, India) was purchased from Thoms Baker, $FeCl_2.4H_2O$ (99%, India) was purchased from Thoms Baker, NH_4OH (25%, Belgium) was purchased from Chem-LAB NV, citric acid (99%, India) was purchased from Thoms Baker, $Al_2(SO_4)_3$ (97%, India) was purchased from HiMedia, NaOH (97%, India) was purchased from HiMedia, HCl (35–38%, India) was purchased from Thoms Baker, distilled water, clay from the Tigris River escarpment were used for the synthesis of MNP1 and MNP2 and for the coagulation and flocculation process.

Synthesis of Fe_3O_4

MNP1 were synthesized by using co-precipitation method. 4.30 g $FeCl_2.4H_2O$ and 11.68 g $FeCl_3.6H_2O$ were dissolved in 200 ml of distilled water in a three neck flask. The flask was equipped with reflux and the solution was bubbled with nitrogen for 10 min after salts were completely dissolved. After that, 45 ml of 25% NH_4OH was added and the reaction mixture was stirred and bubbled for 60 min at 80 °C. After that the black precipitate was washed with distilled water several times until pH reach to 7 followed by drying overnight at 60 °C (Ban et al., 2022).

Synthesis of citric acid coated Fe_3O_4

The MNP1 powder that synthesized previously was dispersed in 200 ml distilled water under sonication and then heated to 90 °C followed by the addition of citric acid. The reaction proceeds for 1 h under stirring and the concentration of citric acid 0.5 g/ml. After that the product MNP2 washed with distilled water several times until pH reaches 7, after that drying the MNP2 overnight at 60 °C (Li et al., 2013).

Characterization technique

Using an Angstrom Advanced Inc ADX2700 X-ray diffractometer, the materials' crystal phase and structure were examined, employing Cu-Kα radiation within the range of 2θ = 10–80°. Using the KBr pellet technique, the samples' Fourier transform infrared (FTIR) spectra were acquired using a Bruker Vector 22 spectrometer between 450 and 4000 cm^{-1}. Field emission scanning electron microscopy (FE-SEM) (Inspect f50 made in Netherlands, FEI company) was used to examine the shape of the MNPs. An EDS system, attached to the FE-SEM, was used for the energy dispersive spectroscopy (EDS) investigation. In addition, atomic force microscopy (Core AFM 2023, Nanosurf AG, Switzerland) was used to examine the shape and size of MNP1 and MNP2. Additionally, the zeta potential of the nanoparticles was examined using Bookhaven 2013, USA.

Coagulation and flocculation experiments

A jar test with six beakers of 500 ml was used for the coagulation and flocculation experiments. The Tigris River water samples with a turbidity of 50 NTU were placed in a volume of 300 ml in each beaker. Different types of coagulants were used in the experiments (Alum, $FeCl_3$, MNP1, and MNP2) with different dosages (10–110 mg/l), and different initial pH values (3–9). Each experimental run was agitated at 200 rpm for 1 min, and then at 50 rpm for 20 min. Then the samples were left to settle for 30 min, and a sample 2 cm from the top was taken to measure the turbidity by a turbidity meter (Lovibond TurbDirect, Germany). The removal efficiency is determined as:

$$Removal\ Efficiency, \% = \left(1 - \frac{C}{C_F}\right) \times 100 \quad (1)$$

where: C is the turbidity after the coagulation and flocculation process, and C_F is the turbidity of the feed solution.

RESULTS AND DISCUSSION

Characterization of magnetic nanoparticles

The mineral phases and crystal sizes of MNP1 and MNP2 were determined using XRD. According to the results, the cubic spinal structure of magnetite was indicated by the diffraction peak positions (2θ = 30.22°, 35.56°, 43.17°, 53.81°, 62.8°, and 62.97°) of MNP1. Similarly, MNP2's (2θ = 30°, 35.55°, 43.4°, 53.9°, 62.85°, and 63.1°) were nearly identical, indicating that the citric acid coating does not cause the phase change of Fe_3O_4 (MNP1) (Singh et al., 2014) as shown in Figure 1. This finding agrees with the peak positions of magnetite reported in Singh et al. (Singh et al., 2014) and Liu et al. (Liu et al., 2018) and JCPDS No. 01-1111.

To find the average size of the crystallites, the Debye-Scherrer equation was utilized:

$$D = \frac{K\,\lambda}{\beta \cos\theta} \tag{2}$$

In this case, θ is the diffraction angle for the peak width at half height, K is a constant of 0.9, and λ is a wavelength of 0.154 nm. Comparing MNP1 and MNP2, the average size of the crystallites was 14.83 nm and 3.51 nm, respectively. This corresponds with the particle size discussed in AFM analysis.

Figure 2 shows the FTIR spectrum of MNP1 and MNP2. The spectra of MNP1 and MNP2 show notable bands at around 583 and 619 cm^{-1}, which are linked to the Fe-O bond. The -OH groups are thought to be responsible for the broad bands observed at 3420 cm^{-1}. The C-H groups are thought to be responsible for the broad bands observed at 2925 and 2854 cm^{-1}. The FTIR spectrum of MNP2 indicated that the citric acid coating on the magnetic nanoparticles was successful because it showed a peak at 1631 cm^{-1}, which corresponds to the C = O bending vibration (symmetric stretching) from the -COOH group of citric acid, and a beak at 1465 cm^{-1}, which corresponds to the asymmetric stretching of C = O from the -COOH group. We attribute the peak of MNP1 and MNP2 at 1113 and 1112 cm^{-1} to C-O stretching. These results were confirmed with Li et al. (Li et al., 2013) and Singh et al. (Singh et al., 2014).

The average particle diameter of MNP1 was 91.51 nm and that of MNP2 was 63.89 nm, as shown in the AFM pictures presented in Figure 3. Because of improvements in dispersion and decreased agglomeration caused by reduced dipole-dipole interactions, surface modification has reduced the size of MNP2 compared to MNP1. These findings are in agreement with the zeta potential values covered in zeta potential section.

Both MNP1 and MNP2 were shown in FE-SEM images in Figure 4. Both MNP1 and MNP2 photos show that the nanoparticles are uniformly shaped and exhibit minimal indications of aggregation. Particle size of MNP2 is smaller than that

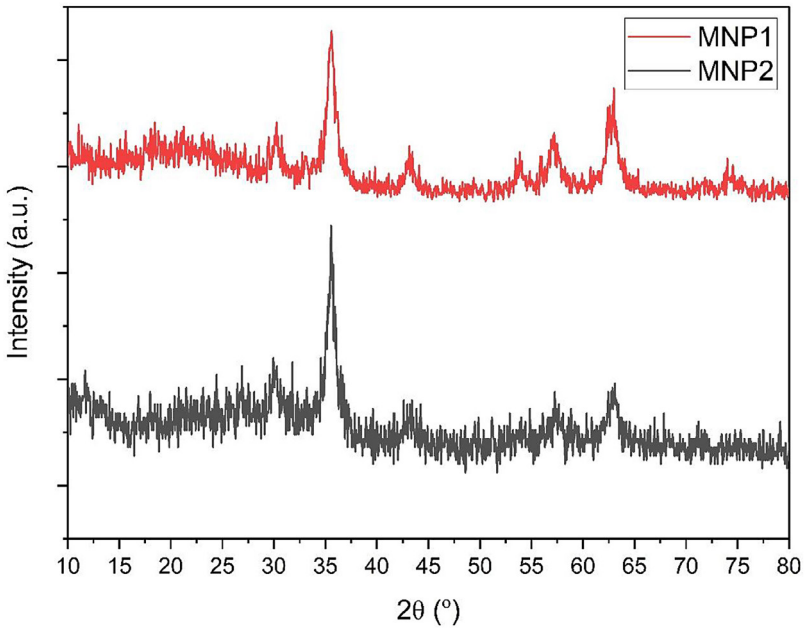

Figure 1. The XRD of MNP1 and MNP2

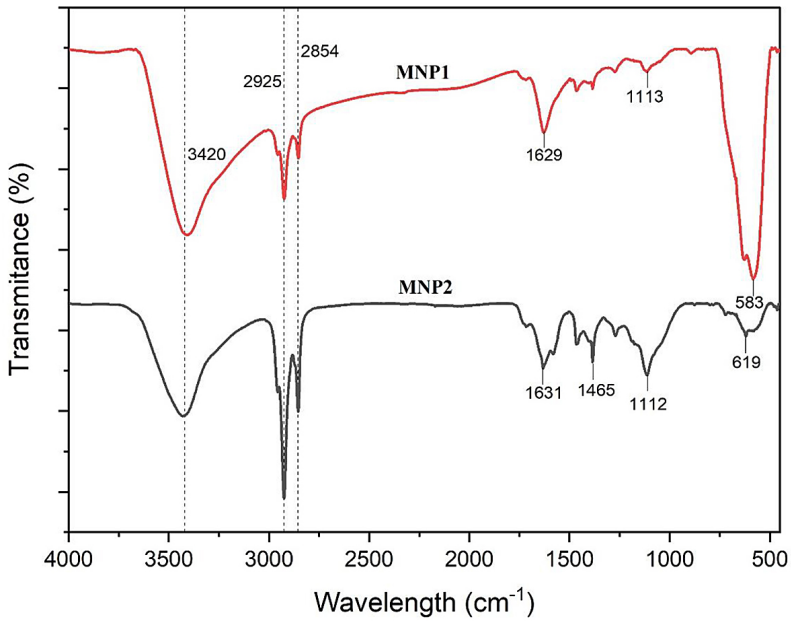

Figure 2. The FTIR of MNP1 and MNP2

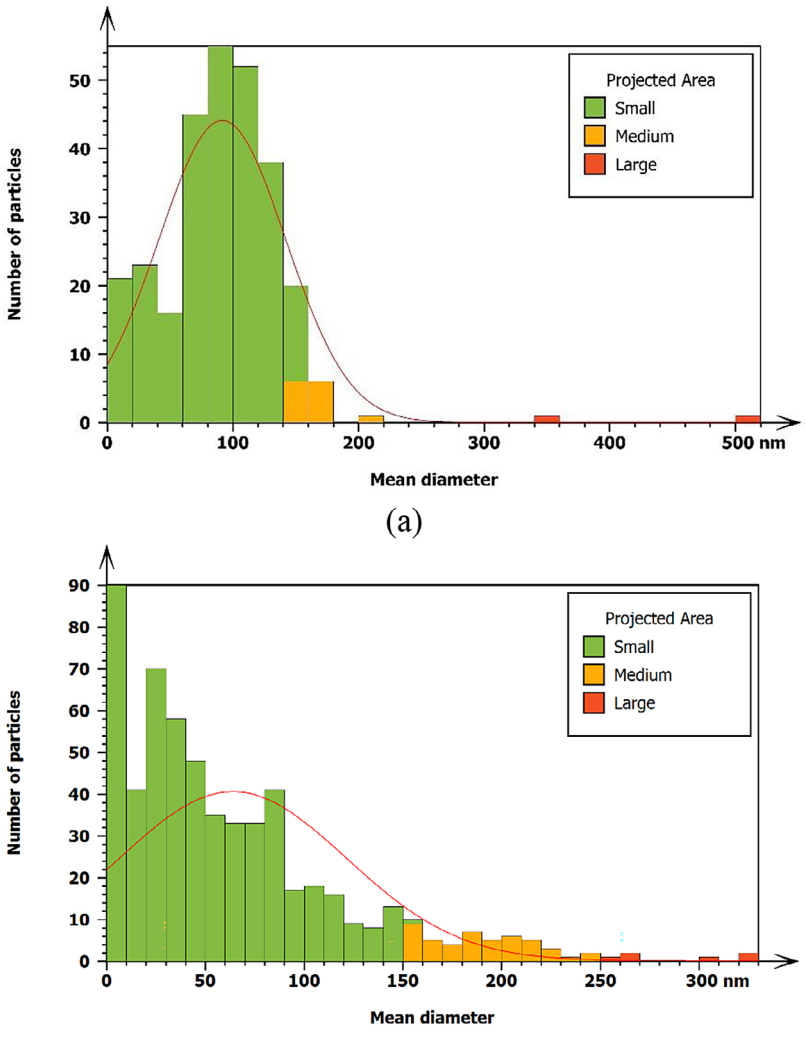

Figure 3. AFM of a) MNP1, and b) MNP2

of MNP1 because, as previously stated, MNP2 exhibits less agglomeration than MNP1, this is illustrated in Figure 4.

The EDS spectra of the synthesized MNP1 was shown in Figure 4a. It was noted that Fe, O, and C were present. The result clearly demonstrated that MNP1 included larger percentages of Fe and O components. Figure 5b shows the EDS spectrum of MNP2, which shows the presence of O, Fe, and C compounds. The fact that the C and O compositions increased and the Fe content dropped (as shown in Figure 4b) suggests that MNP2 was formed when citric acid coated MNP1.

As demonstrated in Figure 5, the surface charges of the MNP1 and MNP2 were determined using zeta potential analysis. According to the findings, their zeta potentials are 31.05 mV and -34.04 mV, respectively. Accordingly, MNP2 is more stable than MNP1, which aggregates more quickly because to its lower absolute zeta potential value. Since MNP1 aggregates quickly, its particle size is greater. One reason is that citric acid's -COOH functional groups can be deprotonated to -COO-. As a result, MNP2 surfaces were significantly negatively charged (Liu et al., 2018).

Coagulation and flocculation process

Since magnetic nanoparticles (MNPs) can be readily regenerated by a magnetic field, their effects on removal efficiency and economic benefits necessitated their investigation. Four coagulants (alum, $FeCl_3$, MNP1, and MNP2) were used to examine the efficiency of coagulation and flocculation process. Results demonstrated that coagulant dosage significantly affected pollutants, and that higher dosages resulted in faster turbidity reduction rates (Figure 6). The removal rate rose to a certain point and then dropped as the dosage was raised. The optimum dosage of alum, $FeCl_3$, MNP1, and MNP2 was 70, 30, 30, and 30 mg/l, respectively. The turbidity removal rate reached 91.28% when the amount of alum as a coagulant was 70 mg/l. The turbidity removal rate reached 96.28% while using 30 mg/l of

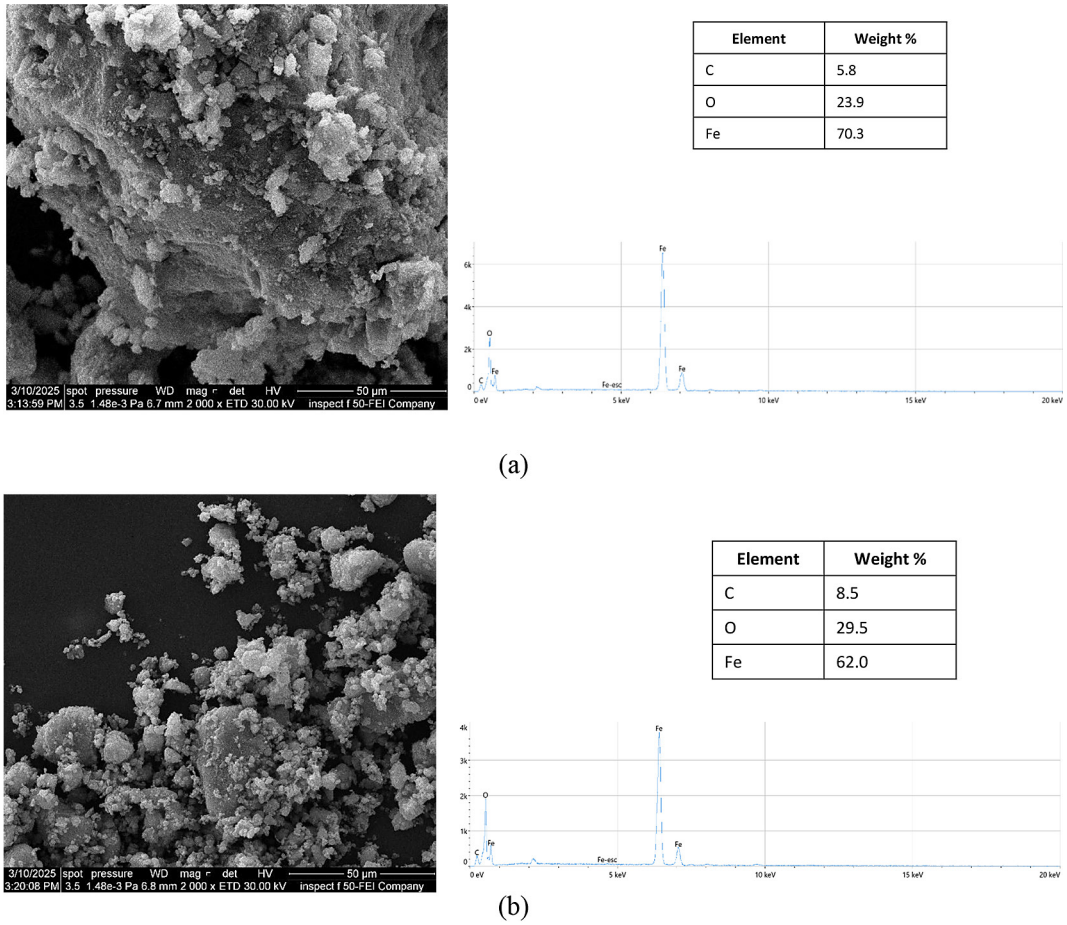

Figure 4. FE-SEM and EDS for a) MNP1, and b) MNP2

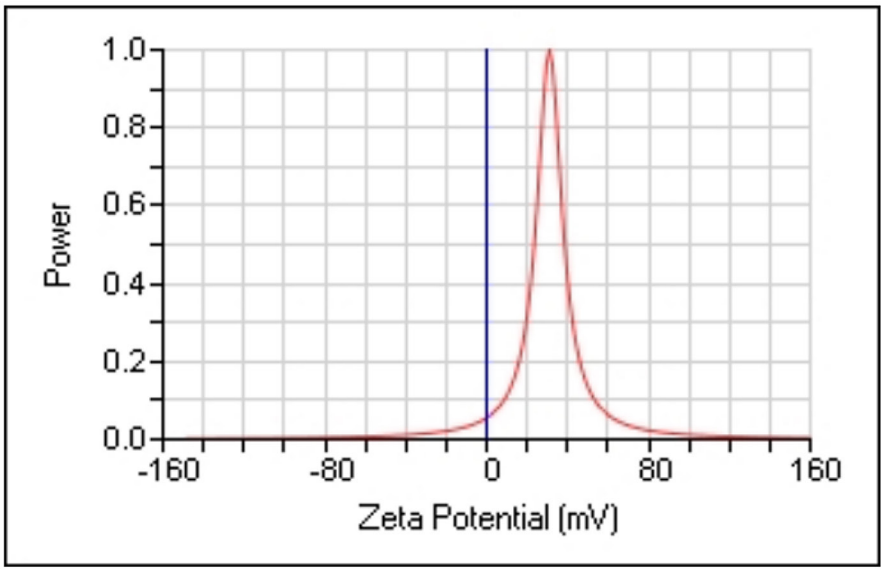

(a)

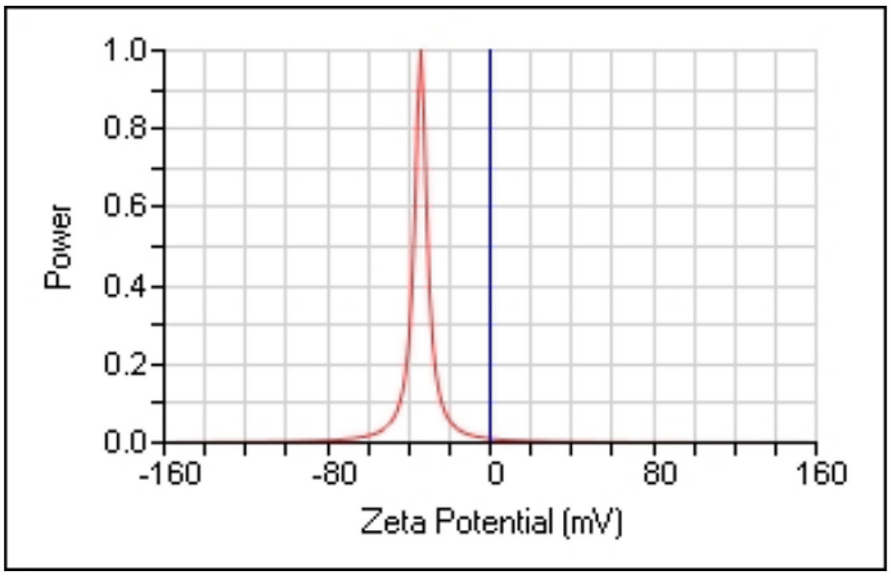

(b)

Figure 5. Zeta potential for a) MNP1, and b) MNP2

$FeCl_3$ as a coagulant. At 30 mg/l, the turbidity removal rate reached 81.46% while using MNP1 as a coagulant. At 30 mg/l, MNP2 demonstrated (highest efficiency) a turbidity removal efficiency of 96.92%.

Within a limited range, increasing the dosage of coagulants, particularly coated MNPs, is equated to increasing the crystal nucleus. MNPs, on the other hand, raise the probability of particle collision and further enhance floc formation. A magnetic copolymer is formed when citric acid-coated MNPs (MNP2) are adsorbed in flocs. This copolymer has a more compact structure and includes more pollutants, leading to improved contaminant removal (Zheng et al., 2020). Overdosing causes destabilization, which in turn causes poor interaction between the pollutant and, according to Stockes' law, a decrease in the settlement velocity of the particles, which in turn causes removal to decline. Increasing the doses typically increases turbidity and decreases removal efficiency. Furthermore, this outcome was

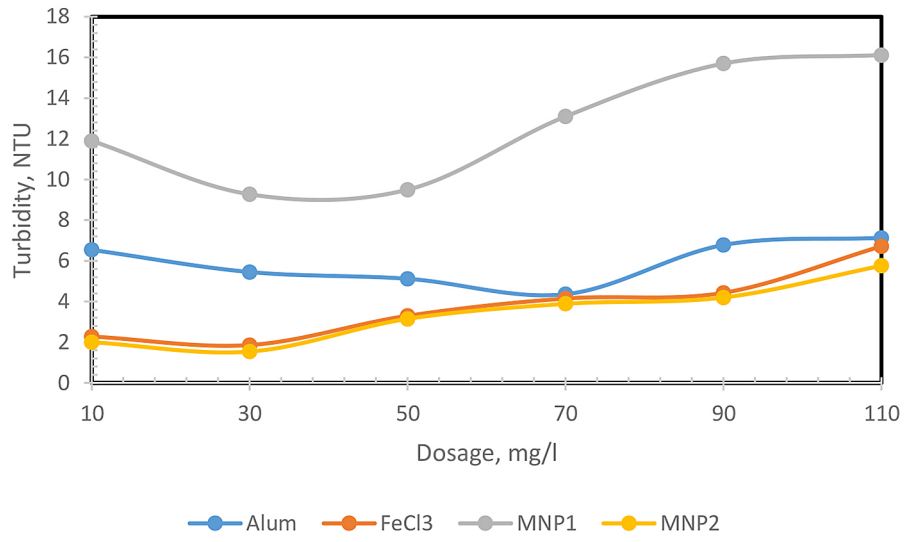

(a)

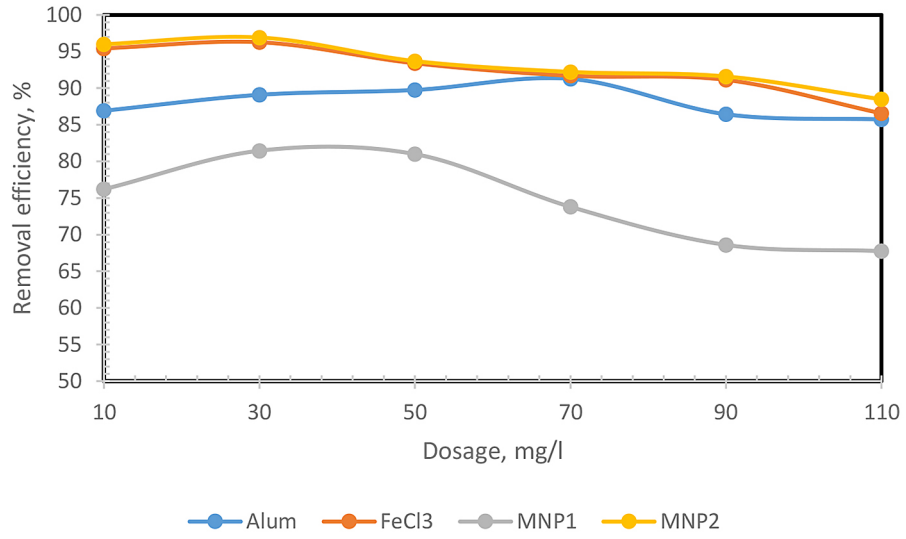

(b)

Figure 6. Effect of coagulant dosage on a) turbidity, and b) removal efficiency

brought about by the following: the flocs' magnetic susceptibility stayed largely unchanged, the coated magnetic nanoparticles reached adsorption saturation on their surface, and an excess of MNPs collided, diminishing the flocculation effect and leading to resource waste.

The removal efficiency reached its highest at pH = 6 and steadily declined when the pH was varied, as illustrated in Figure 7. The maximum removal efficiency of alum (91.28%), FeCl3 (96.28%), MNP1 (81.46%), and MNP2 (96.72%) were observed when the initial pH was 6.0. A lower rate of pollutant removal was observed for starting pH values that were either lower than 6 or higher than 6. Magnetic coagulation's efficacy in removing pollutants is highly sensitive to pH, largely because of the significant impact that pH has on the adsorption performance of magnetic nanoparticles (Tang and Lo, 2013). The zeta potential of the magnetic seeds is affected by the pH, which in turn affects the efficacy of magnetic separation (Serrão Sousa et al., 2017). Because the electrostatic repulsion force increases as the pH rises or falls, changing the pH does little to aid in the removal of pollutants since it raises the surface

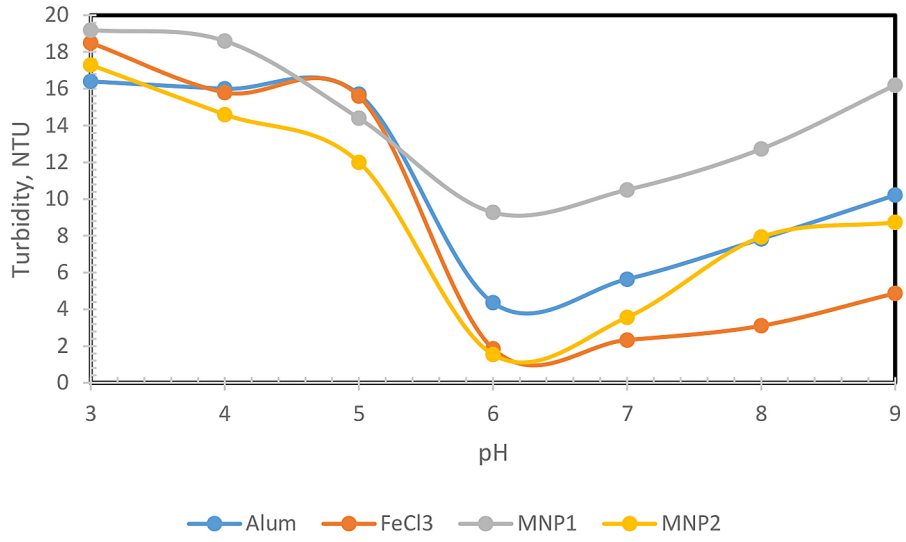

(a)

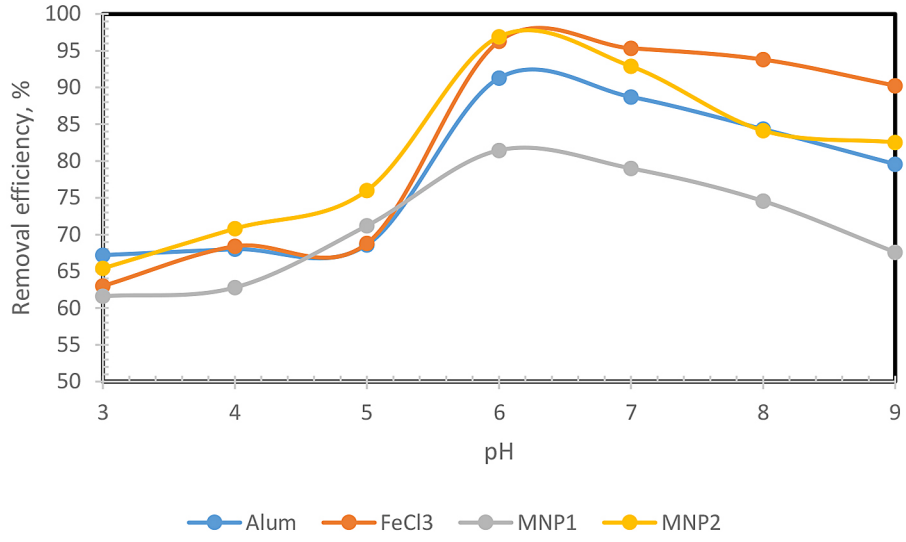

(b)

Figure 7. Effect of pH on a) turbidity, and b) removal efficiency

load of the MNP2. That is why pH 6.0 produced the optimal results.

CONCLUSIONS

The coagulation and flocculation process with synthesized magnetic nanoparticles coated with citric acid was examined on Tigris River water. The results show that MNP2 has a great removal efficiency in coagulation and flocculation process. The characterization confirms successful synthesis of MNP1 and successful coating of citric acid for MNP2. The FTIR analysis demonstrated the formation of a C=O groups resulting from the coating of citric acid on manetic nanoparticles, indicating effective structural integration. The mean diameter of MNP1 and MNP2 were 91.51 nm and 63.89 nm, respectively. The surface charge of MNP1 was positive while, the surface charge of MNP2 was negative. The removal efficiencies of the coagulants have the order of MNP2 > $FeCl_3$ > alum > MNP1, the removal efficiency of MNP2 higher than that of $FeCl_3$, alum, and MNP1 by 0.46%, 6%, and 18.73%, respectively. The optimum initial pH value for four coagulants were 6.

REFERENCES

1. Abdulameer, E. R., Makki, H. F. (2016). Aluminum rubbish as a coagulant for oily wastewater treatment. *Journal of Engineering*, *22*(7), 1–17.
2. Ahmed, M. J., Hameed, B. H., Hummadi, E. H. (2021). Insight into the chemically modified crop straw adsorbents for the enhanced removal of water contaminants: A review. *Journal of Molecular Liquids*, *330*, 115616. https://doi.org/10.1016/j.molliq.2021.115616
3. Al-Madhhachi, A. S. T., Rahi, K. A., Leabi, W. K. (2020). Hydrological impact of ilisu dam on Mosul Dam; the river Tigris. *Geosciences* (*Switzerland*), *10*(4), 1–14. https://doi.org/10.3390/geosciences10040120
4. Al-Rubaie, M. S., Dixon, M. A., Abbas, T. R. (2015). Use of flocculated magnetic separation technology to treat Iraqi oilfield co-produced water for injection purpose. *Desalination and Water Treatment*, *53*(8), 2086–2091. https://doi.org/10.1080/19443994.2013.860400
5. Al-tamimi, N. J., Al-alawy, A. F., Al-shaeli, M. (2025). Evaluation of microfiltration and ultrafiltration membranes for improving water quality : removal of turbidity, suspended solids, and bacteria from the Tigris River. *Iraqi Journal of Chemical and Petroleum Engineering*, *26*(1), 23–34.
6. Algureiri, A. H., Abdulmajeed, Y. R. (2016). Removal of heavy metals from industrial wastewater by using RO membrane. *Iraqi Journal of Chemical and Petroleum Engineering*, *17*(4), 125–136. https://doi.org/10.31699/ijcpe.2016.4.12
7. Ali Abed, S., Hussein Ewaid, S., Al-Ansari, N. (2019). Evaluation of Water quality in the Tigris River within Baghdad, Iraq using multivariate statistical techniques. *Journal of Physics: Conference Series*, *1294*(7). https://doi.org/10.1088/1742-6596/1294/7/072025
8. Alwared, A. I., Faraj, N. S. (2015). Coagulation – flotation process for removing oil from wastewater using Sawdust+ bentonite. *Journal of Engineering*, *21*(6), 62–76. https://doi.org/10.31026/j.eng.2015.06.05
9. Ban, I., Drofenik, M., Bukšek, H., Petrinic, I., Helix-Nielsen, C., Vohl, S., Gyergyek, S., Stergar, J. (2022). Synthesis of magnetic nanoparticles with covalently bonded polyacrylic acid for use as forward osmosis draw agents. *Environmental Science: Water Research and Technology*, *9*(2), 442–453. https://doi.org/10.1039/d2ew00539e
10. Cai, D., Zhang, T., Zhang, F. (2018). Evaluation of oilfield-produced water treated with a prepared magnetic inorganic polymer: Poly(silicate aluminum)/magnetite. *Journal of Applied Polymer Science*, *135*(4), 1–9. https://doi.org/10.1002/app.45735
11. Chen, D., Awut, T., Liu, B., Ma, Y., Wang, T., Nurulla, I. (2016). Functionalized magnetic Fe3O4 nanoparticles for removal of heavy metal ions from aqueous solutions. *E-Polymers*, *16*(4), 313–322. https://doi.org/10.1515/epoly-2016-0043
12. Chen, X., Zheng, H., Xiang, W., An, Y., Xu, B., Zhao, C., Zhang, S. (2019). Magnetic flocculation of anion dyes by a novel composite coagulant. *Desalination and Water Treatment*, *143*, 282–294. https://doi.org/10.5004/dwt.2019.23321
13. Chen, Y., Luo, M., Cai, W. (2016). Influence of operating parameters on the performance of magnetic seeding flocculation. *Environmental Science and Pollution Research*, *23*(3), 2873–2881. https://doi.org/10.1007/s11356-015-5601-5
14. Chhetri, T., Cunningham, G., Suresh, D., Shanks, B., Kannan, R., Upendran, A., Afrasiabi, Z. (2022). Wastewater treatment using novel magnetic nanosponges. *Water (Switzerland)*, *14*(3), 1–12. https://doi.org/10.3390/w14030505
15. Deivasigamani, P., Gajendiran, V., Chitra, B., Kumar, P. S., Balasubramanian, N., Sundararaman, S., Dhananjeyan, V., Subramani, L., Jagadeesan, A. K., Sivamani, S., Chellappa, R., Rangasamy, G. (2025). Magnetic nanoparticles: synthesis, characterization and application based on environmental perspective. *Results in Chemistry*, *14*(December 2024), 102023. https://doi.org/10.1016/j.rechem.2025.102023
16. Demissie, H., An, G., Jiao, R., Ritigala, T., Lu, S., Wang, D. (2021). Modification of high content nanocluster-based coagulation for rapid removal of dye from water and the mechanism. *Separation and Purification Technology*, *259*, 117845. https://doi.org/10.1016/j.seppur.2020.117845
17. Dhakal, N., Salinas-Rodriguez, S. G., Hamdani, J., Abushaban, A., Sawalha, H., Schippers, J. C., Kennedy, M. D. (2022). Is desalination a solution to freshwater scarcity in developing countries? *Membranes*, *12*(4), 1–15. https://doi.org/10.3390/membranes12040381
18. Dhamin, J. Z., Majeed, N. S. (2022). Removal of Heavy Metal Ions from Wastewater Using Bulk Liquid Membrane Technique Enhanced by Electrical Potential. *AIP Conference Proceedings*, *2660*(April). https://doi.org/10.1063/5.0109421
19. Farajnezhad, H., Gharbani, P. (2012). Coagulation treatment of wastewater in petroleum industry using poly aluminium chloride and ferric chloride. *IJRRAS*, *13*(1), 306–310.
20. Gao, J., Zhu, W., Yan, Y., Yue, Z., Guo, X. (2022). Application of magnetic coagulation for the advanced treatment of ethylene glycol wastewater. *Desalination and Water Treatment*, *246*, 146–155. https://doi.org/10.5004/dwt.2022.28014
21. Hatamie, A., Parham, H., Zargar, B., Heidari, Z. (2016). Evaluating magnetic nano-ferrofluid as a

novel coagulant for surface water treatment. *Journal of Molecular Liquids*, *219*, 694–702. https://doi.org/10.1016/j.molliq.2016.04.020

22. Hu, Z., Wu, K., Wang, Z., Shah, K. J., Sun, Y. (2024). Research progress of magnetic flocculation in water treatment. *Magnetochemistry*, *10*(8). https://doi.org/10.3390/magnetochemistry10080056
23. Jamaly, S., Giwa, A., Hasan, S. W. (2015). Recent improvements in oily wastewater treatment: Progress, challenges, and future opportunities. *Journal of Environmental Sciences*, *37*, 15–30. https://doi.org/10.1016/j.jes.2015.04.011
24. Kadhim, H., Al-alawy, A. F., Rashid, T., Al-mosawi, A. I., Salih, M. H. (2024). Mathematical modeling of osmotic membrane bioreactor process for oily wastewater treatment. *Water Science and Technology*, *90*(7), 2234–2250. https://doi.org/10.2166/wst.2024.318
25. Khujamberdiev, R., Cho, H. M. (2025). Synthesis and Characterization of Nanoparticles in Transforming Biodiesel into a Sustainable Fuel. *Molecules*, *30*(6). https://doi.org/10.3390/molecules30061352
26. Li, L., Mak, K. Y., Leung, C. W., Chan, K. Y., Chan, W. K., Zhong, W., Pong, P. W. T. (2013). Effect of synthesis conditions on the properties of citric-acid coated iron oxide nanoparticles. *Microelectronic Engineering*, *110*, 329–334. https://doi.org/10.1016/j.mee.2013.02.045
27. Liu, J., Dai, C., Hu, Y. (2018). Aqueous aggregation behavior of citric acid coated magnetite nanoparticles: Effects of pH, cations, anions, and humic acid. *Environmental Research*, *161*(October 2017), 49–60. https://doi.org/10.1016/j.envres.2017.10.045
28. Lv, M., Li, D., Zhang, Z., Logan, B. E., Peter van der Hoek, J., Sun, M., Chen, F., Feng, Y. (2021). Magnetic seeding coagulation: Effect of Al species and magnetic particles on coagulation efficiency, residual Al, and floc properties. *Chemosphere*, *268*, 129363. https://doi.org/10.1016/j.chemosphere.2020.129363
29. Mardani, S., Aghabalaei, V., Tabeshnia, M., Baghdadi, M. (2021). Modification of conventional coagulation–flocculation process with graphene oxide and magnetite nanoparticles for turbidity removal from surface water. *Desalination and Water Treatment*, *229*, 206–216. https://doi.org/10.5004/dwt.2021.27393
30. Mohamed Noor, M. H., Wong, S., Ngadi, N., Mohammed Inuwa, I., Opotu, L. A. (2022). Assessing the effectiveness of magnetic nanoparticles coagulation/flocculation in water treatment: a systematic literature review. *International Journal of Environmental Science and Technology*, *19*(7), 6935–6956. https://doi.org/10.1007/s13762-021-03369-0
31. Mohammadtabar, F., Khorshidi, B., Hayatbakhsh, A., Sadrzadeh, M. (2019). Integrated coagulation-membrane processes with zero liquid discharge (ZLD) configuration for the treatment of oil sands produced water. *Water*, *11*, 1–12. https://doi.org/10.3390/w11071348
32. Mohammed, T. J., Abbas, E. R. (2017). Turbidity and Oil Removal from Oilfield Produced Water, by Coagulation - Flocculation Technique. *The Eighth Jordan International Chemical Engineering Conference (JIChEC 2017)*, 1–8. https://doi.org/10.1051/matecconf/201816205010
33. Mohammed, T. J., Shakir, E. (2018). Effect of settling time, velocity gradient, and camp number on turbidity removal for oilfield produced water. *Egyptian Journal of Petroleum*, *27*(1), 31–36. https://doi.org/10.1016/j.ejpe.2016.12.006
34. Msemwa, G. G., Nasr, M., Abdelhaleem, A., Fujii, M., Ibrahim, M. G. (2025). Coagulation-flocculation/pyrolysis integrated system for dye-laden wastewater treatment: a techno-economic and sustainable approach. *Water, Air, and Soil Pollution*, *236*(1), 1–21. https://doi.org/10.1007/s11270-024-07659-4
35. Mustereț, C. P., Morosanu, I., Ciobanu, R., Plavan, O., Gherghel, A., Al-Refai, M., Roman, I., Teodosiu, C. (2021). Assessment of coagulation–flocculation process efficiency for the natural organic matter removal in drinking water treatment. *Water (Switzerland)*, *13*(21). https://doi.org/10.3390/w13213073
36. Organization, W. H. (2011). Guidelines for Drinking-Water Quality. In *World Health Organization*.
37. Ritigala, T., Chen, Y., Zheng, J., Demissie, H., Zheng, L., Yu, D., Sui, Q., Chen, M., Zhu, J., Fan, H., Li, J., Gao, Q., Weragoda, S. K., Weerasooriya, R., Jinadasa, K. B. S. N., Wei, Y. (2021). Comparison of an integrated short-cut biological nitrogen removal process with magnetic coagulation treating swine wastewater and food waste digestate. *Bioresource Technology*, *329*(January). https://doi.org/10.1016/j.biortech.2021.124904
38. Ritigala, T., Demissie, H., Chen, Y., Zheng, J., Zheng, L., Zhu, J., Fan, H., Li, J., Wang, D., Weragoda, S. K., Weerasooriya, R., Wei, Y. (2021). Optimized pre-treatment of high strength food waste digestate by high content aluminum-nanocluster based magnetic coagulation. *Journal of Environmental Sciences (China)*, *104*, 430–443. https://doi.org/10.1016/j.jes.2020.12.027
39. Salih, M. H., Al-Alawy, A. F. (2022). Crystallization process as a final part of zero liquid discharge system for treatment of East Baghdad oilfield produced water. *Iraqi Journal of Chemical and Petroleum Engineering*, *23*(1), 15–22. https://doi.org/10.31699/ijcpe.2022.1.3
40. Salih, M. H., Al-Alawy, A. F., Ahmed, T. A. (2021). Oil skimming followed by coagulation/flocculation processes for oilfield produced water treatment and zero liquid discharge system application. *AIP*

Conference Proceedings, *2372*, 060006. https://doi.org/10.1063/5.0065365

41. Salih, M. H., Hassan, H. A., Al-Alawy, R. M., Zaboon, S., Al-Alawy, A. F., Al-Jendeel, H. A. (2024). Green power generation from the Tigris River using pressure retarded osmosis process. *Desalination and Water Treatment*, *320*(November), 100887. https://doi.org/10.1016/j.dwt.2024.100887
42. Serrão Sousa, V., Corniciuc, C., Ribau Teixeira, M. (2017). The effect of TiO_2 nanoparticles removal on drinking water quality produced by conventional treatment C/F/S. *Water Research*, *109*, 1–12. https://doi.org/10.1016/j.watres.2016.11.030
43. Singh, D., Gautam, R. K., Kumar, R., Shukla, B. K., Shankar, V., Krishna, V. (2014). Citric acid coated magnetic nanoparticles: Synthesis, characterization and application in removal of Cd(II) ions from aqueous solution. *Journal of Water Process Engineering*, *4*(C), 233–241. https://doi.org/10.1016/j.jwpe.2014.10.005
44. Soros, A., Amburgey, J. E., Stauber, C. E., Sobsey, M. D., Casanova, L. M. (2019). Turbidity reduction in drinking water by coagulation-flocculation with chitosan polymers. *Journal of Water and Health*, *17*(2), 204–218. https://doi.org/10.2166/wh.2019.114
45. Stiufiuc, G. F., Stiufiuc, R. I. (2024). Magnetic nanoparticles: synthesis, characterization, and their use in biomedical field. *Applied Sciences (Switzerland)*, *14*(4). https://doi.org/10.3390/app14041623
46. Tang, S. C. N., Lo, I. M. C. (2013). Magnetic nanoparticles: Essential factors for sustainable environmental applications. *Water Research*, *47*(8), 2613–2632. https://doi.org/10.1016/j.watres.2013.02.039
47. Zheng, L., Jiao, Y., Zhong, H., Zhang, C., Wang, J., Wei, Y. (2020). Insight into the magnetic lime coagulation-membrane distillation process for desulfurization wastewater treatment: From pollutant removal feature to membrane fouling. *Journal of Hazardous Materials*, *391*(December 2019), 122202. https://doi.org/10.1016/j.jhazmat.2020.122202
48. Zhou, Z., Shan, A., Zhao, Y. (2017). Synthesis of a novel magnetic polyacrylamide coagulant and its application in wastewater purification. *Water Science and Technology*, *75*(3), 581–586. https://doi.org/10.2166/wst.2016.500